International Journal of Chemical, Materials and Biomolecular Sciences
ISSN: 2415-6620
Vol:5, No:9, 2011

The Incorporation of In in GaAsN as a Means of N Fraction Calibration

H. Hashim, and B. F. Usher

***Abstract*—**InGaAsN and GaAsN epitaxial layers with similar nitrogen compositions in a sample were successfully grown on a GaAs (001) substrate by solid source molecular beam epitaxy. An electron cyclotron resonance nitrogen plasma source has been used to generate atomic nitrogen during the growth of the nitride layers. The indium composition changed from sample to sample to give compressive and tensile strained InGaAsN layers. Layer characteristics have been assessed by high-resolution x-ray diffraction to determine the relationship between the lattice constant of the $GaAs_{1-y}N_y$ layer and the fraction x of In. The objective was to determine the In fraction x in an $In_xGa_{1-x}As_{1-y}N_y$ epitaxial layer which exactly cancels the strain present in a $GaAs_{1-y}N_y$ epitaxial layer with the same nitrogen content when grown on a GaAs substrate.

***Keywords*—**Indium, molecular beam epitaxy, nitrogen, strain cancellation.

I. Introduction

SINCE Kondow et al [1] experimented on InGaAsN as a candidate for near infra-red devices (1.3 to 1.55 μm) grown on GaAs substrates, considerable work by others has followed (e.g. [2]-[5]). By adding a small amount of nitrogen to GaAs and InGaAs there is a decrease in both the bandgap energy and the lattice parameter [6], [7]. While there have been many reports of the electronic and optical properties of GaAsN and InGaAsN alloys, there have been few studies of methods of determining nitrogen fractions in these materials (e.g. [8]-[10]).

In this paper, we study strain cancellation in GaAsN epitaxial layers by the addition of In as a method for calibrating N fractions. Preliminary results of this study have been reported previously [11] with the same N fractions of about 0.003 for nitride layers in all four samples examined. This work reports an extension of earlier work by the growth of several sets of samples containing higher N fractions of about 0.006, 0.007, 0.01 and 0.011. The idea is to take a tensile layer of GaAsN which exhibits a particular perpendicular lattice constant, which is measured accurately by HRXRD, and determine the fraction x of In which must replace Ga to exactly cancel the tensile strain in the layer. The fraction x is found where $In_xGa_{1-x}As_{1-y}N_y$ – GaAs peak separations plotted against varying In fraction x passes through zero arcseconds, equivalent to exact lattice matching of the layer to the substrate.

H. Hashim is with the Department of Electronic Engineering, La Trobe University, Victoria 3086, Australia (phone: 61-3-94791920; e-mail: hhashim@students.latrobe.edu.au).

B. F. Usher is with the Department of Electronic Engineering, La Trobe University, Victoria 3086, Australia (e-mail: b.usher@latrobe.edu.au).

II. Experimental Procedure

The experiments were performed in a highly modified Varian molecular beam epitaxy (MBE-360) system. Substrates were degreased and etched using semiconductor grade chemicals and indium soldered onto molybdenum substrate holders before being loaded into the system. Substrates were oriented vertically in the growth chamber, which was pumped by a 400 l/s ion pump to give a residual gas pressure less than 10^{-9} Torr. The Ga, In and arsenic (As_4) fluxes originated from boron nitride crucibles in effusion cells and their temperatures were set to achieve the desired fluxes for each sample.

The MBE growth of dilute nitrides on GaAs (001) substrates commonly uses a radio frequency (RF) plasma source to produce atomic nitrogen. However, in this work an electron cyclotron resonance (ECR) plasma source was used to provide active N radicals from a pure (99.9999%) N_2 gas. There are several benefits in using an ECR plasma source instead of an RF plasma source, as described in [12], [13]. This work used a 2.45 GHz microwave generator and operated with a constant plasma current of 12 or 18 mA, depending on the nitrogen flux required, with a 50V ion trap to eliminate charged species from the beam. The nitrogen gas flow rate was adjusted with a leak valve and its pressure in the chamber was monitored via the mass 28 peak from a quadrupole mass spectrometer (QMS) or via the ion pump current which measured the high background N_2 pressure, assured to correlate reasonably with the atomic nitrogen flux. The nitrogen pressure was assumed constant for each sample.

The substrate was slowly heated to remove the oxide from the surface under an As_4 flux and this process was monitored in situ using reflection high energy electron diffraction (RHEED). The substrate temperature was measured by a thermocouple positioned close to, but not touching, the back of the substrate. Following oxide removal, the substrate was held at an elevated temperature for about 15 minutes to ensure the oxide layer had been completely removed. The Ga shutter was then opened for about 5 minutes for the growth of a GaAs buffer layer at this substrate temperature, known from experience to be approximately 600°C. The substrate temperature was then reduced slowly in order to observe the RHEED pattern transition between the 2x4 and c(4x4) surface reconstructions, known to occur at a temperature of 530°C [14]. This calibration process allowed determination of the indicated temperature at which the real substrate temperature was 600°C for GaAs growth and 540°C for the growth of layers containing indium or nitrogen. A GaAs buffer layer was then grown at a 600°C equivalent temperature at a rate of approximately 1 ML/s for about 10 minutes after which the Ga

flux was determined by monitoring the RHEED intensity oscillations observed following initiation of GaAs growth.

The sample structure was similar for all samples, consisting of individual InGaAsN and GaAsN layers as well as a 10 period InGaAs/GaAs multi quantum well (MQW). They were grown on 500 μm thick GaAs (001) substrates as shown in Fig. 1. The $In_xGa_{1-x}As$/GaAs MQW was designed to allow calibration of the Ga and In fluxes from which the In fraction x could be determined. The In fraction was assumed to be the same in the MQW as in the InGaAsN layer and the N fraction was also assumed to be the same in the GaAsN and InGaAsN layers. There are two buffer layers of thickness 160 nm between the InGaAsN and GaAsN, and GaAsN and InGaAs/GaAs MQW layers and temperature changes were made during the growth of these layers so there were no growth interruptions. This ensured that the InGaAsN, GaAsN and InGaAs/GaAs MQW layers were grown at the design temperature of 540°C where evaporative loss of In and N is negligible. The thicknesses of the InGaAsN and GaAsN layers were designed to be lower than their critical thicknesses as determined from the force-balance model of Matthews and Blakeslee [15]. This was important to avoid misfit dislocation formation in the layer interfaces which would result in a loss of interfacial coherence, an important assumption on which the analysis has been based. The InGaAsN layer thicknesses were between 200 and 400 nm while the GaAsN layer thicknesses were between 50 and 100 nm. The buffer layer thicknesses were not as critical as those of the epitaxial layers.

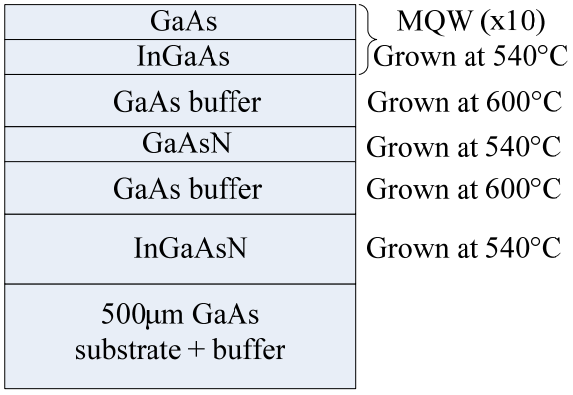

Fig. 1 The structure of all samples with layer thicknesses omitted.

We grew five sets of samples with various N fractions which were designated sets 1, 2, 2b, 3 and 3b. The N fraction was designed to be increased from one set of samples to another. Each set was intended to consist of four samples, two containing compressively strained InGaAsN layers and two with InGaAsN layers in tension, however set 3b consisted of only two samples. The layer strain was adjusted by changing the In furnace temperature and therefore the In flux. Sets one and two were grown at a low nitrogen plasma current of 12mA with the nitrogen pressure stabilized by setting the QMS multiplier current to 4.5×10^{-9} Amps when tuned to the N_2 peak. For the higher N compositions, growths were performed at a higher nitrogen plasma current of 18 mA and the nitrogen pressure in the growth chamber was stabilized by monitoring the ion pump current. The higher background nitrogen pressure in the chamber during operation of the plasma source meant that nitrogen was the dominant species contributing to the pressure. Therefore a higher nitrogen plasma power was required to grow samples at higher N compositions to limit the pressure the ion pump was exposed to. Another problem was that the sensitivity of the QMS was also compromised at high N pressures. Set 2b was grown to repeat the results of set 2 and set 3b was grown to repeat the results of set 3 but with the higher nitrogen plasma current of 18 mA.

For the growth of $Ga_{1-x}As_{1-y}N_y$, the Ga incorporation rate I_{Ga} can be related to the As and N incorporation rates I_{As} and I_N by:

$$I_{Ga} = I_{As} + I_N . \quad (1)$$

The relationship between incorporation rates and N fraction y is given by:

$$\frac{I_N}{I_{As}} = \frac{y}{1 - y}. \quad (2)$$

From (1) and (2), y could be related to the N and Ga incorporation rates by:

$$y = \frac{I_N}{I_{Ga}}. \quad (3)$$

If the sticking coefficients of N and Ga are unity (confirmed by experiment [12], [13], [16]), incorporation rates can be replaced by flux rates so:

$$y = \frac{\gamma_N}{\gamma_{Ga}}. \quad (4)$$

This shows that the N fraction is expected to be inversely proportional to the Ga flux γ_{Ga}, and so the atomic fraction y of N could be increased by reducing the Ga growth rate at constant N flux γ_N. Each set was designed to have a constant Ga flux in order to yield the same N fraction in all samples within a set.

It was necessary to structurally characterize each sample to determine their In content by collecting the (004) HRXRD spectra from the reference InGaAs/GaAs MQW grown on the top of each sample. The HRXRD measurements were performed using a system equipped with a parabolic multilayer mirror and a four-bounce Ge (220) Bartels monochromator and used a conventional x-ray generator with a copper target as the radiation source ($Cu_{K\alpha 1}$, λ=1.54060Å) operating in line focus mode. When all data on the InGaAs/GaAs MQW had been collected, the MQW structure was etched from each sample to avoid the complications in the HRXRD spectra caused by the InGaAs/GaAs MQW peaks

overlapping with the peaks originating from the single InGaAsN and GaAsN layers. The samples were etched in a polishing etchant consisting of H_2SO_4(96%):H_2O_2(30%):H_2O mixed in the volume proportions 8:1:1. The H_2O_2 and the H_2O were premixed in the proportions 1:1 and both this mixture and the H_2SO_4 were mixed and then stored at 4°C to cool the etchant following the exothermic reaction that occurs when they are mixed and which increases the etch rate and makes it less predictable. The etch rate was calibrated from step height measurements using an Atomic Force Microscope (AFM). Following the removal of the InGaAs/GaAs MQW structures, each sample was again subjected to HRXRD measurement to obtain a spectrum that consisted only of the GaAs substrate peak and the individual InGaAsN and GaAsN layer peaks.

III. Results and Discussions

Fig. 2 shows (004) rocking curves from four of the samples having two N fractions. Samples S1070311 and S2090311 had N fractions of about 0.007 while samples S1100211 and S2310111 contained N fractions of about 0.01. The spectra show clear zero and higher order satellite peaks from the InGaAs/GaAs MQW layers as labelled in the figure. All InGaAsN layer peaks are labelled as X in the figure. Samples S1070311 and S2090311 contained compressive and tensile strained InGaAsN layers respectively. The compressive InGaAsN layer peak is to the left of the GaAs substrate peak while the tensile layer peak is to the right of the GaAs substrate peak. The tensile InGaAsN layer peak for sample S2310111 is very close to the GaAs substrate peak and the compressive InGaAsN layer peak is between the GaAs substrate and the zeroth order MQW peak for sample S1100211. The GaAsN layer peaks for all samples are to the right of the GaAs substrate peak.

HRXRD measurements on the samples were collected at azimuthal (Phi) angles of 0°, 90°, 180° and 270° for each sample to identify any layer tilts. Layer tilts can occur for a number of reasons, including a slight miscut of the (001) substrate or the presence of misfit dislocations. Any simple tilt effects can be seen from this data with the peak separations between the GaAs substrate and zeroth order peak of the InGaAs/GaAs MQW following a sine function with an amplitude equal to the tilt angle. This is important since the HRXRD simulation software used in this work did not allow the inclusion of layer tilts in the simulation. The Phi angle at which the sine function equals its average gives a condition at which the tilt has no effect on the spectrum and a HRXRD scan was repeated at this angle to give a fifth spectrum. From the fifth spectrum the In fraction could be calculated from the InGaAs/GaAs MQW. This value of In fraction had therefore been corrected for tilt effects and this procedure was repeated for all samples. The value of the In fraction obtained from the fifth HRXRD spectrum was then used to fit simulations to experimental rocking curve spectra collected at Phi of 0°, 90°, 180° and 270° following removal of the InGaAs/GaAs MQW layers.

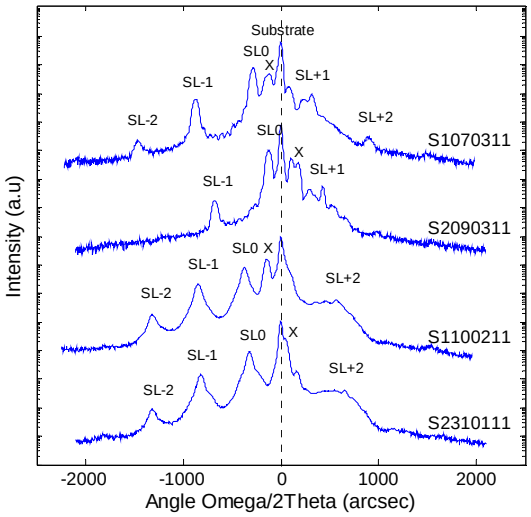

Fig. 2 XRD rocking curves.

After removal of the InGaAs/GaAs MQW layers the HRXRD measurements were repeated. Examples of HRXRD spectra obtained after removal of the InGaAs/GaAs MQW are shown in Fig. 3. The GaAsN peaks are clearly observed although broad in the high N fraction samples S1100211 and S2310111. The GaAsN peak is broad since it originates from a thin layer and therefore it is difficult to identify its angular separation relative to the GaAs substrate. InGaAsN-GaAs and GaAsN-GaAs peak separations obtained at four azimuthal angles were again fitted to a sine function.

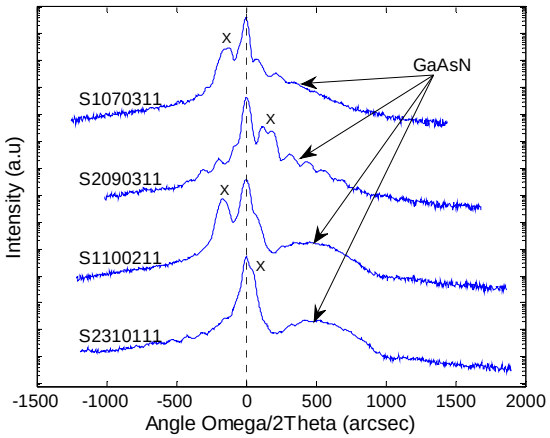

Fig. 3 XRD rocking curves after removal of the InGaAs/GaAs MQW.

The experimental HRXRD curves were compared with dynamical simulations to determine the angular separations between the InGaAsN and GaAs substrate peaks and between the GaAsN and GaAs peaks as shown in Fig. 4 for sample S1100211. The compressively strained InGaAsN layer peak is on the left of the GaAs substrate while the GaAsN peak is on the right of the substrate. Some of the fringes in the simulation

are not seen in the experimental curve, suggesting some interfacial roughness even though the calculated thicknesses of each layer were less than their critical thicknesses. Following simulation, the thickness of the GaAsN layer could be increased to give a clear GaAsN peak allowing ready measurement of its separation from the GaAs substrate peak and therefore an estimated N fraction y could be calculated based on this separation.

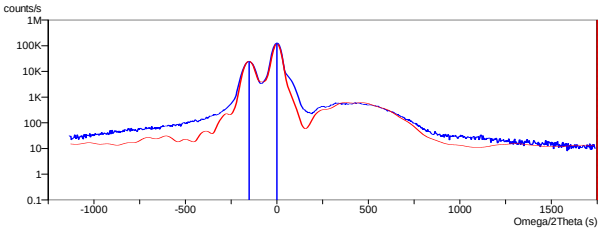

Fig. 4 XRD rocking curve and dynamical theory simulation from sample S1100211.

Simulation based on dynamical x-ray diffraction theory is also very useful to identify the InGaAsN-GaAs peak separation when the InGaAsN layer peak was very close to the substrate and not clearly resolved. For example the InGaAsN-GaAs layer peak separation for sample S2310111 could be found following simulation by increasing the InGaAsN layer thickness until its angular position was clear. Then from its lattice spacing, it was possible to calculate the perpendicular lattice constant of InGaAsN layer by the same method as was used for the GaAsN layer. The lattice constants and elastic parameters of GaAs, InAs, GaN and InN that were used in the calculations are shown in Table I [17], [18]. Assuming coherent interfaces the parallel lattice constant of all layers were assumed to be identical to the GaAs substrate and Poisson's ratio v was assumed equal to that of the GaAs substrate 0.322 [19]. This is because the nitrogen fractions are low, of the order of 0.3% to 1.2% and the Indium fractions are also low, expected to be about three times these fractions. Therefore all layers are very close to the composition of GaAs and so this assumption would seem reasonable in the absence of better data on Poisson's ratio.

TABLE I
THE PARAMETER VALUES

Parameter	GaAs	InAs	GaN	InN
Lattice constant, a_0 (Å)	5.65325	6.0583	4.5	4.98
Elastic constant, C_{11} (10^{11}N/m^2)	1.174	0.833	2.93	1.87
Elastic constant, C_{12} (10^{11}N/m^2)	0.526	0.453	1.59	1.25

The results from all samples in each set are summarized in Table II. The values of the In fraction x shown in the table were found from an analysis of the $In_xGa_{1-x}As$/GaAs MQWs by the method explained above and in [20]. The negative sign of the InGaAsN-GaAs peak separations in Table II indicate the InGaAsN layers were on the left side of the GaAs substrate and therefore compressively strained. For tensile InGaAsN layers when the peaks are on the right side of the GaAs substrate, their peak separations have a positive sign. The estimated values of N fraction y in Table II were calculated from the GaAsN-GaAs peak separations and are only estimates of the N composition of each sample. The values of x at which the separation between InGaAsN layer and GaAs substrate peaks should be zero were determined from the plots in Fig. 5. The plot allows determination of x required to exactly cancel the strain in a GaAsN layer of known perpendicular d-spacing. The errors in determined the peak positions from all HRXRD spectra were about ±3.5 arcsec as shown in the table and this contributes an error in the In fraction of about ±0.001.

TABLE II
THE EXPERIMENTAL RESULTS

Set	Sample	$\theta_{InGaAsN}$ - θ_{GaAs} (±3.5 arcsec)	θ_{GaAsN} - θ_{GaAs} (±3.5 arcsec)	x (±0.001)	y (±0.0001) (Estimate)	x at $\theta_{InGaAsN}$-θ_{GaAs}=0 (±0.001)
1	S2071009	+35.1	184.7	0.008	0.0035	0.009
	S1011209	-111.3	205.2	0.017	0.0038	
	S2011209	-93.7	183.8	0.015	0.0034	
	S4011209	+52.1	168.2	0.006	0.0031	
2	S1280110	-171.8	229.4	0.022	0.0043	0.017
	S2280110	+96.2	414.3	0.017	0.0077	
	S1290110	-115.7	278.9	0.022	0.0052	
	S2290110	-46.6	322.8	0.020	0.0060	
2b	S1070311	-137.6	383.3	0.029	0.0072	0.021
	S2070311	+86.5	375.7	0.015	0.0070	
	S1090311	-48.7	394.5	0.025	0.0074	
	S2090311	+155.7	388.2	0.013	0.0073	
3	S2310111	+40.2	637.8	0.032	0.0119	0.033
	S1020211	-183.3	608.7	0.043	0.0114	
	S1100211	-152.5	526.4	0.037	0.0098	
	S2100211	+95.0	526.6	0.024	0.0098	
3b	S1230211	-65.3	637.7	0.039	0.0119	0.035
	S2230211	+106.0	492.2	0.021	0.0092	

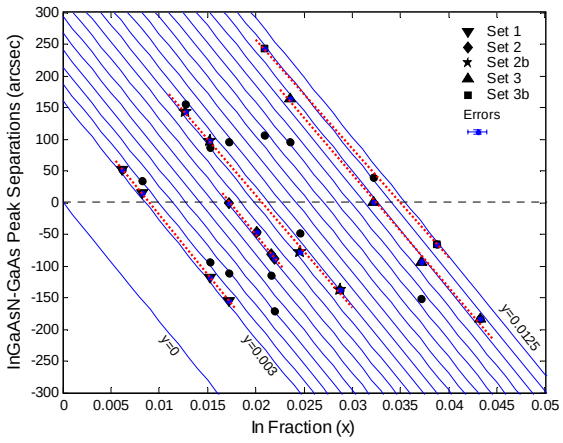

Fig. 5 A plot of InGaAsN-GaAs peak separations against x for various values of y. The y values are estimates only, based on assumptions that Poisson's ratio and lattice constants are known and Vegard's law holds

The theoretical relationship between InGaAsN-GaAs peak separations and In fraction x at various N fraction can be developed as follows. From Bragg's law, the observed angle of the (004) reflection from a tetragonally distorted crystal with perpendicular lattice constant, $a^{\perp}$ is given by:

$$\theta = \sin^{-1}\left(\frac{2\lambda}{a^{\perp}}\right). \quad (5)$$

By assuming the InGaAsN layers obey Vegard's Law, the natural lattice constant of an InGaAsN layer is given by:

$$a_{In_xGa_{1-x}N_yAs_{1-y}} = xya_{InN} + y(1-x)a_{GaN} + x(1-y)a_{InAs} + (1-x)(1-y)a_{GaAs} \quad (6)$$

where x is the atomic fraction of In and y is the atomic fraction of N.

Linear elasticity theory allows us to relate the natural lattice constant a of a layer to its parallel $a^{\parallel}$ and perpendicular $a^{\perp}$ lattice constants through:

$$a = \frac{2v}{1+v}a^{\parallel} + \frac{1-v}{1+v}a^{\perp} \quad (7)$$

where v is Poisson's ratio for the material. If all interfaces in a sample are coherent, the parallel lattice constant of each layer will be the same as the parallel lattice constant of the GaAs substrate. Since all values in (7) depend on v, any change in v will modify this equation and thus the theoretical relationship between InGaAsN-GaAs peak separations and In fraction x at various N fraction y also will be different. Therefore it is important to know the accurate value of the v for the InGaAsN layers.

By combining (5), (6) and (7) and substituting parameters from Table I we obtained:

$$\theta = \sin^{-1}\frac{1.58022}{x(0.40505 + 0.07495y) - 1.15325y + 2.89932} \quad (8)$$

Hence, the peak separations between InGaAsN layer and GaAs substrate are given by:

$$\theta_{InGaAsN} - \theta_{GaAs} = \theta - 33.02682439 \quad (9)$$

where $\theta_{InGaAsN}$ and θ_{GaAs} are the Bragg angles associated with the InGaAsN layer and the GaAs substrate peaks. A plot of InGaAsN-GaAs peak separations against In fraction x for various theoretical N fractions y are shown in Fig. 5. All solid circle data points in the plot are the experimental data from samples in Table II, while the others are scaled data, obtained as described below.The diagonal lines in the plot are theoretical lines for y equal to zero and values between 0.003 and 0.0125 at increments of 0.0005. The horizontal line in the plot represents zero peak separation between an InGaAsN and a GaAs layer. From this plot it can be seen that some points are above the zero peak separation line and others are beneath it, corresponding to tensile and compressively strained InGaAsN layers. Although the experiments were intended to have consistent N fluxes for all samples in each set it was not the same as it was difficult to achieve constant N fluxes for all samples grown over one or two days. Therefore, a scaling method was applied to each experimental data point relative to a selected experimental data point so that all data points would lie on the same N fraction line, allowing a line of best fit to be plotted through all four data points for each set of samples as shown in the figure. The line of best fit for each set gives the In equivalent of the N fraction in the GaAsN layer for which the InGaAsN epitaxial layer would be exactly lattice matched to the GaAs substrate. By a similar process as that which resulted in (9), the peak separations between GaAsN layer and GaAs substrate at different In fractions are given by:

$$\theta_{GaAsN} - \theta_{GaAs} = \theta' - 33.02682439 \quad 10)$$

where θ' is the Bragg angle associated with a $GaAs_{1-y}N_y$ layer. Therefore a theoretical relationship between GaAsN-GaAs peak separation and x can be plotted as shown in Fig. 6. The theoretical line was plotted for various values of Poisson's ratio between 0.3 and 0.33. Each data point in the plot represents a set of samples as labelled in the figure. The value of x for each data point is the amount of In required to exactly cancel the strain in an GaAsN layer and GaAsN-GaAs peak separations are the experimental data from the sample selected as the standard to which other samples within the set were scaled. From Fig. 6, it is clear that it is important to know Poisson's ratio in order to establish a relationship between the GaAsN-GaAs peak separations and the In fraction. The data appears to match theory if the value of Poisson's ratio is about 0.31. This theoretical relationship will be changed if the values of the lattice constants for GaN and InN tabulated in Table I are not accurate, likely since literature values quote those to only two or three significant figures.

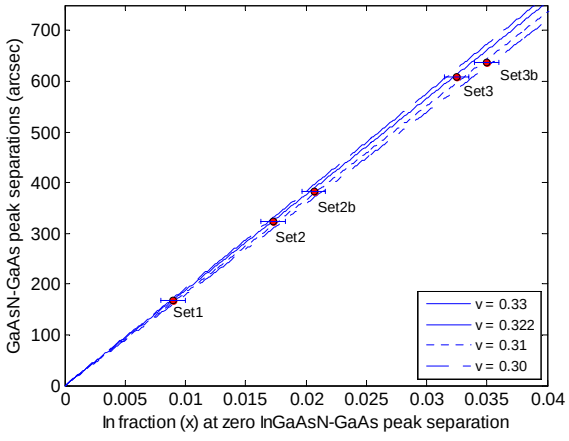

Fig. 6 Plot of GaAsN-GaAs peak separations versus In fraction x.

IV. Conclusions

We have presented a simple approach to determine the amount of In required to exactly cancel the strain in a GaAsN layer in order to calibrate the N fraction. Based on the results reported in this paper, it is important to investigate Poisson's ratio of GaAsN, so the relationship between In and N fractions at which the strain has been exactly cancelled in an InGaAsN quaternary alloy can be determined. However uncertainties in GaN and InN lattice constants could also explain discrepancies between theory and experiment and the assumption that Vegard's law holds is also untested in this material system. The next step in this study is to determine the values of Poisson's ratio for the various N fractions studied to date.

Acknowledgment

The authors wish thank to the University of Technology MARA Malaysia and the Ministry of Higher Education Malaysia for their financial support.

References

[1] M. Kondow, K. Uomi, A. Niwa, T. Kitatani, S. Watahiki, and Y. Yazawa, "GaInNAs: A novel material for long-wavelength-range laser diodes with excellent high-temperature performance,"*Japanese Journal of Applied Physics, Part 1 (Regular Papers, Short Notes & Review Papers),* vol. 35, pp. 1273-1275, 1996.

[2] M. Montes, A. Guzman, A. Trampert, and A. Hierro, "1.3 μm emitting GaInNAs/GaAs quantum well resonant cavity LEDs," *Solid-State Electronics,* vol. 54, pp. 492-496, Apr 2010.

[3] A. Khadour, S. Bouchoule, G. Aubin, J. C. Harmand, J. Decobert, and J. L. Oudar, "Ultrashort pulse generation from 1.56 μm mode-locked VECSEL at room temperature," *Optics Express,* vol. 18, pp. 19902-19913, Sep 2010.

[4] S. M. Wang, H. Zhao, G. Adolfsson, Y. Q. Wei, Q. X. Zhao, J. S. Gustavsson, M. Sadeghi, and A. Larsson, "Dilute nitrides and 1.3 μm GaInNAs quantum well lasers on GaAs," *Microelectronics Journal,* vol. 40, pp. 386-391, March 2009.

[5] Y. Qu, H. Li, J. X. Zhang, B. X. Bo, X. Gao, and G. J. Liu, "High performance 1.3 μm InGaAsN superluminescent diodes," *Science in China Series E-Technological Sciences,* vol. 52, pp. 2396-2399, Aug 2009.

[6] M. Weyers, M. Sato, and H. Ando, "Red shift of photoluminescence and absorption in dilute GaAsN alloy layers," *Japanese Journal of Applied Physics, Part 2 (Letters),* vol. 31, pp. L853-L855, July 1992.

[7] M. Weyers and M. Sato, "Growth of GaAsN alloys by low-pressure metalorganic chemical vapor deposition using plasma-cracked NH_3," *Applied Physics Letters,* vol. 62, pp. 1396-1398, March 1993.

[8] W. Lu, J. J. Lim, S. Bull, A. V. Andrianov, C. Staddon, C. T. Foxon, M. Sadeghi, S. M. Wang, A. Larsson, and E. C. Larkins, "Independent determination of In and N concentrations in GaInNAs alloys," *Semiconductor Science and Technology,* vol. 24, pp. 4, Oct 2009.

[9] J. Serafinczuk and J. Kozlowski, "Determination of indium and nitrogen content in four-component epitaxial layers of $In_xGa_{1-x}As_{1-y}N_y$ deposited on GaAs substrate," *Materials Science,* vol. 26, pp. 207-212, 2008.

[10] Q. X. Zhao, S. M. Wang, M. Sadeghi, A. Larsson, M. Friesel, and M. Willander, "Nitrogen incorporation in GaNAs layers grown by molecular beam epitaxy," *Applied Physics Letters,* vol. 89, pp. 3, Jul 2006.

[11] H. Hashim and B. F. Usher, "Strain cancellation by indium incorporation for the calibration of nitrogen fractions in GaAsN," in *2010 IEEE International Conference on Semiconductor Electronics*, pp. 8-11, June, 2010.

[12] B. F. Usher, T. Warminski, T. Dieing, and K. Prince, "Characterisation of a nitrogen ECR plasma source for the MBE growth of the dilute nitride semiconductor GaAsN," *Surface Science,* vol. 601, pp. 5800-5802, Dec 2007.

[13] B. Usher, T. Warminski, T. Dieing, and K. Prince, "High temperature growth of the dilute nitride GaAsN using a nitrogen ECR plasma source," *2006 International Conference on Nanoscience and Nanotechnology (IEEE Cat. No.06EX1411),* pp. 4, 2007.

[14] T. Dieing, "MBE growth of GaAsN using an ECR plasma source," PhD Thesis, La Trobe University, 2005, pp.77.

[15] J. W. Matthews and A. E. Blakeslee, "Defects in epitaxial multilayers. I. Misfit dislocations," *Journal of Crystal Growth,* vol. 27, pp. 118-125, Dec 1974.

[16] T. M. Brennan, J. Y. Tsao, and B. E. Hammons, "Reactive sticking of As_4 during molecular beam homoepitaxy of GaAs, AlAs, and InAs, "*Journal of Vacuum Science & Technology a-Vacuum Surfaces and Films,* vol. 10, pp. 33-45, Jan-Feb 1992.

[17] O. Madelung, M. Schulz, and H. Weiss, "Technology of III-V, II-VI and non-tetrahedrally bonded compounds," in *Landolt Börnstein (Numerical Data and Functional Relationships in Science and Technology)*. vol. 17, K. H. Hellwege and O. Madelung, Eds.: Springer, Berlin, 1984, pp. 13-14.

[18] I. Vurgaftman, J. R. Meyer, and L. R. Ram-Mohan, "Band parameters for III-V compound semiconductors and their alloys," *Journal of Applied Physics,* vol. 89, pp. 5815-5875, Jun 2001.

[19] B. F. Usher, D. Zhou, S. C. Goh, T. Warminski, and X. P. Huang, "Poisson's ratio of GaAs," in *Proc. Optoelectronic and Microelectronic Materials Devices,* 1998, pp. 290-293.

[20] B. F. Usher and D. Zhou, "Thickness and composition determination of MBE grown strained multiple quantum well structures by x-ray diffraction," *Proceedings of the SPIE - The International Society for Optical Engineering,* vol. 4086, pp. 76-81, 2000.